Parity Violation Observed in the Beta Decay of Magnetically Trapped ^{82}Rb Atoms

S. G. Crane,[1,2] S. J. Brice,[1] A. Goldschmidt,[1] R. Guckert,[1] A. Hime,[1] J. J. Kitten,[1] D. J. Vieira,[1] and X. Zhao[1]

[1]*Los Alamos National Laboratory, Los Alamos, New Mexico 87545*

[2]*Department of Physics, Utah State University, Logan, Utah 84322*

(Received 18 October 2000)

Laser cooling and atomic trapping techniques have been employed to confine polarized ^{82}Rb atoms ($T_{1/2} = 75$ s) in a magnetic time-orbiting-potential (TOP) trap. We have observed the parity-violating correlation between the emitted positron momentum and the parent nuclear spin as a continuous function of angle and positron energy for this pure Gamow-Teller (GT) transition. These proof-of-principle measurements demonstrate the utility of exploring fundamental symmetries in a TOP trap and the steps required to improve sensitivity in the search for physics beyond the standard model.

DOI: 10.1103/PhysRevLett.86.2967 PACS numbers: 23.40.Bw, 27.50.+e, 29.25.Rm, 32.80.Pj

Of the four fundamental forces in nature the weak interaction is unique in that it violates parity, or space-reflection symmetry. More than four decades have passed since the first suggestion by Lee and Yang that parity could be violated in weak interactions [1] and the subsequent discovery in the beta decay of polarized ^{60}Co nuclei [2]. Today, maximal violation of parity (and of charge-conjugation) symmetry is accommodated in the standard model describing a pure vector-axial vector (V-A) helicity structure for weak interactions. This model was developed largely upon the empirical observations of nuclear beta decay during the latter half of the past century [3]. Despite the phenomenological success of the standard model, the fundamental origin of parity violation is unknown. Nuclear beta decay experiments continue to serve as a probe of the origin of parity violation and, more generally, the helicity structure of the weak interaction [4].

One manifestation of parity violation in nuclear beta decay is the asymmetry in the angular distribution of the beta particles emitted relative to the spin orientation of the parent nucleus. Pure Gamow-Teller (GT) transitions offer a direct route to study parity violation because they proceed solely through the axial-vector coupling in the standard model. To date, the most precise measure of the beta-spin correlation coefficient (known as A) from a pure GT decay comes from a modern experiment using polarized ^{60}Co nuclei [5]. In that experiment the angular dependence of the asymmetry was verified by measuring the relative electron intensity at a set of discrete angles. A value of $A = -1.01 \pm 0.02$ was deduced for the correlation coefficient in agreement with expectations for a pure GT, electron emitter with $\triangle J = -1$. Given the difficulty in reducing the systematic uncertainties associated with absolute polarization and electron scattering effects in a solid sample, improved precision appears unlikely using such technology. The advent of laser cooling [6], magnetic [7], and magneto-optical [8] trapping of neutral atoms offers a new approach for isolating and confining a cold and effectively massless, radioactive source. A number of new generation experiments are now being pursued that exploit atom trapping technologies to study fundamental symmetries [9].

At Los Alamos, we have mounted an experiment to study the positron-spin correlation in ^{82}Rb beta decay by exploiting the unique features of a time-orbiting-potential (TOP) trap [10]. Our goal is to explore possible deviations from maximal parity violation using this new technology. The TOP trap offers the ability to confine a highly polarized sample of atoms in a cloud of the order of 1 mm in diameter. A key feature for this experiment is the magnetic bias field that defines a polarization vector for the trapped sample and which rotates uniformly in an equatorial plane. This produces a rotating beacon of spin-polarized nuclei that can be used to measure the positron-spin correlation as a continuous function of positron momentum and emission angle using a single positron detector. Mapping the correlation function in this continuous fashion is of significance since one can utilize both dipole (asymmetry) and quadrupole (anisotropy) terms in the angular distribution to measure recoil order corrections that are difficult to estimate beyond the allowed approximation when breaching the 1% level of precision [11].

We use $\sim$10 mCi of ^{82}Sr ($T_{1/2} = 26$ d), which decays by electron capture into ^{82}Rb ($T_{1/2} = 75$ s) to provide a long-lived, off-line parent source for our short-lived species of interest. The ^{82}Sr sample is placed in the ion source of a mass separator which selectively ionizes, mass separates, and implants the ^{82}Rb daughter into a Zr foil that is located inside the primary trapping cell (see Fig. 1). Subsequent heating of the implantation foil releases ^{82}Rb atoms as a dilute vapor into the trapping cell where they are cooled and trapped by a magneto-optical trap (MOT) (see Ref. [12], for more details). The trapped ^{82}Rb atoms are then transferred through an 11 mm diameter, 40 cm long tube using a short pulse of laser light with magnetic confinement along the tube axis [13] to guide the atoms into a second, high-vacuum chamber housing the positron detector. The transferred atoms are retrapped in a second MOT and then prepared for loading into the TOP trap.

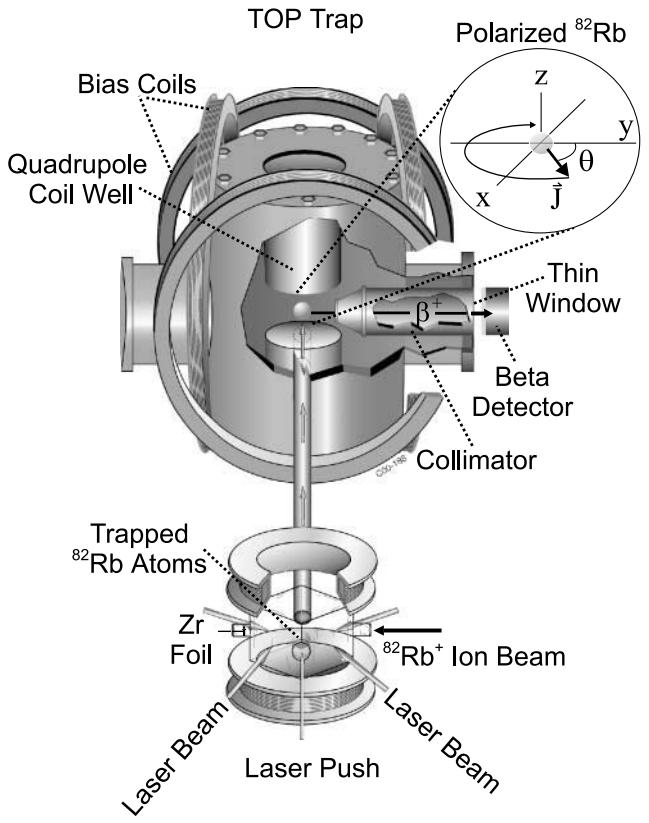

FIG. 1. Experimental system for producing a trapped and polarized source of ^{82}Rb (not drawn to scale). The atoms are trapped by a MOT in the glass cell, then transferred and loaded into a TOP trap in the second chamber. The TOP quadrupole field gradient is generated by anti-Helmholtz coils (not shown) located inside the quadrupole coil wells. Two pairs of Helmholtz coils are driven with a relative phase of 90° to produce the rotating bias magnetic field that is tracked by the sample polarization vector in the x-y plane. Positrons from the decay of ^{82}Rb emitted along the y axis are detected by the plastic scintillator.

Once retrapped in the second MOT, the atoms are further cooled using an optical molasses [14] and then optically pumped into the $5S_{1/2}(F = 3/2, m_F = 3/2)$ ground state. This electron-nuclear spin stretched state ensures that the nuclear spin is aligned with the local magnetic field. The TOP trap confines the atom in a quadrupole field gradient ($\partial B/\partial \rho = 40$ G/cm) to which an 830 Hz rotating bias field of 15 G is added. The rotation frequency is small compared to the Larmor precession frequency of the atom; consequently the nuclear spin adiabatically follows the bias magnetic field. Monte Carlo calculations indicate that this choice of field settings is appropriate to achieve polarization as high as 96% while ensuring that a false asymmetry associated with magnetic deflection of positrons is smaller than 0.2%. We are able to trap as many as 500 000 ^{82}Rb atoms in a single loading of the TOP trap.

Positrons are detected in a plastic scintillator (76 mm diameter and 20 mm thick) after they pass through a thin (50 μm) stainless steel window that separates the detector from the second chamber vacuum, which is maintained at less than 3×10^{-11} torr. Passive collimators are employed to define the full opening angle for positron detection of 18.2°. An event in the plastic scintillator triggers the data acquisition electronics to record the energy deposited in the plastic, the MOT fluorescence signal, and the coil currents that produce the quadrupole and rotating bias field. From the recorded bias coil currents we construct the direction of the average nuclear spin for each positron event up to a phase shift arising from the resistive skin effect. This phase shift has been measured using a Hall probe to be 131° ± 2° (zero phase occurs in the absence of the metal chamber). Data are collected in a cyclic fashion where we run through the entire sequence of implantation, release, trapping, transfer, optical pumping, TOP loading, and detection as described above. For each cycle we detect the decay of atoms in the TOP trap for 60 s. Typical positron detector and MOT fluorescence signals are shown in Fig. 2.

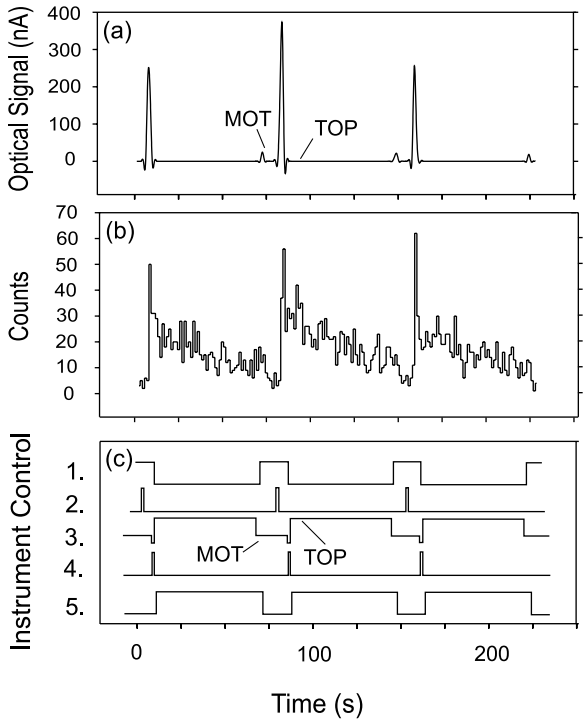

FIG. 2. (a) Fluorescence and (b) beta decay data collected using a 60 s detection interval. The large spikes in the MOT fluorescence signal, measured by a photomultiplier tube, indicate a successful MOT-to-MOT transfer of ^{82}Rb into the second chamber. The fluorescence abruptly drops when the MOT trapping light is turned off as the TOP magnetic trap is loaded. At this point the beta decay signal drops by half, indicating ~50% loading efficiency into the TOP trap. Beta-asymmetry data are accumulated from this point until the residual atoms are momentarily retrapped in a MOT just before the next cycle begins. (c) Typical time sequencing showing the on/off pulsing of (1) MOT lasers; (2) MOT-to-MOT transfer pulse; (3) quadrupole current (notice MOT and TOP levels); (4) molasses cooling and optical pumping; (5) bias coils and counting period.

In order to study the angular distribution the data were binned according to the angle (θ) between the nuclear spin and the emitted positron momentum after integrating over the positron energy [see Fig. 3(a)]. The data are well described by a $1 + \alpha\cos(\theta)$ distribution with a preponderance of positrons emitted in the same direction as the nuclear spin, which is expected for ^{82}Rb positron decay. These data distinctly demonstrate the successful confinement of a rotating, nuclear-polarized sample of ^{82}Rb in a TOP trap.

For ^{82}Rb there are two dominant transitions that have positron-spin correlation coefficients of $A^{1^+\to 0^+} = 1$ (branching ratio = 86.4%) and $A^{1^+\to 2^+} = -1/2$ (12.6%) [15] in the standard model (i.e., a V-A interaction). The measured angular distribution can be written as

$$N(\theta) = S\big(1 + PG\langle\beta A\rangle\cos(\theta + X)\big) + B\,,$$

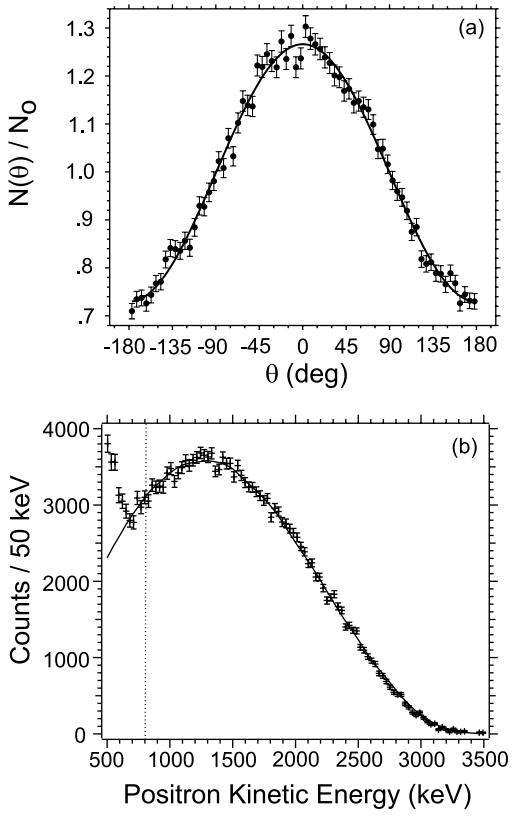

FIG. 3. ^{82}Rb beta decay data accumulated over a period of 6 h. (a) The angular distribution obtained after binning the events as a function of positron-spin angle (phase shift removed) and integrating over the positron energy above a threshold of 800 keV. The solid line results from a cosine fit to the distribution from the trapped sample data. (b) The differential positron energy spectrum obtained after integrating over the observed emission angle θ instead. The solid curve is computed assuming an allowed ^{82}Rb spectrum including the two-component decay scheme and folding in the experimental response function. The spectrum departs from a pure positron signal at low energy due to Compton scattering of 776 keV gamma rays from the 2^+ state of the ^{82}Kr daughter.

where S is the signal arising from the TOP trap with an average nuclear polarization P, and G is a geometric factor that arises after averaging the cosine function over the finite solid angle of the detector ($G = 0.994$). $\langle\beta A\rangle$ is the product of positron velocity relative to light and the asymmetry amplitude for the multibranch decay of ^{82}Rb averaged over positron energy. The phase shift (X) extracted from the data of $133.4° \pm 0.5°$ is in good agreement with independent measurements using the Hall probe. An uncorrelated background (B) arises from events that are detected but that do not originate from the trapped sample. It is convenient to rewrite the distribution as $N(\theta) = N_0[1 + \alpha\cos(\theta)]$, where $\alpha = (1 + B/S)^{-1}\langle\beta A\rangle PG$, and $N_0 = S + B$. A cosine fit to the observed angular distribution [Fig. 3(a)] yields $\alpha = 0.268 \pm 0.004$. In the standard model we compute $\langle\beta A\rangle = 0.80$ (using a positron energy threshold of 800 keV), indicating a nonzero background and/or polarization less than 100%.

The uncorrelated background is dominated by ^{82}Rb atoms that are lost in the trapping process and make their way to the walls of the chamber where they subsequently beta decay from an unpolarized state. Positrons can be detected from the walls when ^{82}Rb atoms find their way to the surface of the quadrupole coil wells or the thin window in front of the positron detector. Positrons originating at the quadrupole well do not have a direct line of sight to the detector but can still be detected if they scatter from the inside surface of the collimator. Two processes in which atoms are lost to the walls of the chamber give rise to separate background components. In the first place, losses occur due to inefficiencies in the MOT-to-MOT and MOT-to-TOP transfer processes (B_1). A second component (B_2) arises when atoms are lost due to the finite trap lifetime (measured to be 70 s). To determine the background associated with loading inefficiency (B_1) we recorded an independent data sample by loading the TOP trap and then immediately dropping the trap by switching off the quadrupole field. In order to study the effects of the finite trap lifetime, another data sample was recorded while extending the decay detection interval from 60 to 250 s. The observed temporal decay departs from a single exponential and yields the combined contribution from B_1 and B_2. Analysis of these background experiments yields $B_1/S = 0.41 \pm 0.02$ and $B_2/S = 0.37 \pm 0.03$. A third, time-independent component (B_3) arises due to ambient background in the laboratory and is determined from measurements without ^{82}Rb transferred to the second chamber to be $B_3/S = 0.110 \pm 0.004$.

Because we do not yet have the means to independently determine the sample polarization P, the extraction of the positron-spin correlation coefficient from the data was not possible. However, by using the total signal-to-background ratio ($B/S = 0.89 \pm 0.04$) along with the standard model value for $\langle\beta A\rangle$ of 0.80, we deduce a global nuclear polarization of $64 \pm 2\%$ for our ^{82}Rb sample.

By integrating the data over the observed emission angle, we produce an unpolarized sample and thus the differential energy spectrum for positrons. The spectrum is shown in Fig. 3(b) after subtracting the background components described above. Also shown is the Monte Carlo derived spectrum expected for ^{82}Rb decay after folding in the energy-dependent response function for positrons in the apparatus. The simulation includes energy loss effects associated with scattering in the passive collimator and the thin window, backscattering and bremsstrahlung in the plastic scintillator, summing of 511 keV annihilation radiation in the plastic scintillator, and the intrinsic energy resolution of the detector. The data agree well with the assumption of an allowed shape and indicate that experimental distortions are under control. From this we deduce that the known instrumental effects, if not taken into account, would cause a systematic shift when extracting the positron-spin correlation coefficient that is smaller than 1%.

Analysis of these proof-of-principle experiments clearly points to several requirements and improvements to make a high-precision measurement of the positron-spin correlation coefficient in ^{82}Rb. Reduction of uncorrelated background can be accomplished with improvements in the trap loading efficiency and lifetime. We are also working to implement new detector hardware that will identify positrons that annihilate in the plastic scintillator and which originate from the trap region. Ultimately, the background can be largely eliminated by extracting the recoil ion in coincidence with the detected positron [16]. This would also allow for the simultaneous measurement of other correlation coefficients depending on the neutrino degrees of freedom. Clearly, an independent measurement of the polarization is required in order to extract the positron-spin correlation coefficient from the data. We are currently working to image the trapped sample, which provides information on the position distribution and temperature of atoms in the cloud. Together with a measurement of the magnetic field over the trap region, we will be able to determine the polarization of the trapped sample. Models of the atom cloud indicate that at 20 μK (a temperature that has been achieved using molasses cooling on stable Rb atoms [10]) we can expect polarization greater than 96% with our current experimental setup. The present polarization of 64% suggests that improvements are required to optimize the optical molasses and optical pumping procedures. In addition, atomic fluorescence techniques will be applied to directly measure the atomic m-state population.

In summary, we have demonstrated the feasibility of a new method to study parity violation in nuclear beta decay using a TOP trap. We have recorded the parity violating, positron-spin correlation as a continuous function of positron energy and emission angle. The angular distribution and differential energy spectrum are consistent with allowed ^{82}Rb decay and our knowledge of the positron response function. We have also developed techniques to measure the uncorrelated background and the information gained will be invaluable in reducing background in future experiments. Analysis of these proof-of-principle experiments indicates that, with sufficient reduction of background and an independent measure of polarization, the positron-spin correlation coefficient could be extracted at the 1% level of precision and beyond. Future experiments can then improve the search for physics beyond the standard model that might arise in the presence of right-handed and/or tensor coupling.

We are grateful to T. J. Bowles, E. A. Cornell, M. Di Rosa, S. Lamoreaux, D. Tupa, and C. E. Weiman for many useful discussions and suggestions. Particular thanks go to M. Anaya, W. Artcher, R. Mier, A. D. Montoya, F. J. Hauser, W. Teasdale, J. Smith, and especially L. D. Benham for providing excellent technical support. This work is supported in large part by the Laboratory Directed Research and Development program at Los Alamos National Laboratory, operated by the University of California for the U.S. Department of Energy.

[1] T. D. Lee and C. N. Yang, Phys. Rev. **104**, 254 (1956).
[2] C. S. Wu *et al.,* Phys. Rev. **105**, 1413 (1957).
[3] R. E. Marshak, Riazuddin, and C. P. Ryan, in *Theory of Weak Interactions in Particle Physics,* edited by R. E. Marshak, Monagraphs and Texts in Physics and Astronomy Vol. 24 (Wiley, New York, 1969).
[4] P. Herczeg, in *Precision Tests of the Standard Electroweak Model,* edited by P. Langacker, Advanced Series on Directions in High Energy Physics Vol. 14 (World Scientific, Teaneck, NJ, 1995); J. Deutsch and P. Quin, *ibid.*
[5] L. M. Chirovsky *et al.,* Phys. Lett. **94B**, 127 (1980).
[6] W. D. Phillips and H. Metcalf, Phys. Rev. Lett. **48**, 596 (1982).
[7] A. L. Migdall *et al.,* Phys. Rev. Lett. **54**, 2596 (1985).
[8] E. L. Raab *et al.,* Phys. Rev. Lett. **59**, 2631 (1987).
[9] Z. T. Lu *et al.,* Phys. Rev. Lett. **72**, 3791 (1994); G. Gwinner *et al.,* Phys. Rev. Lett. **72**, 3795 (1994); J. A. Behr *et al.,* Phys. Rev. Lett. **79**, 375 (1997).
[10] W. Petrich *et al.,* Phys. Rev. Lett. **74**, 3352 (1995).
[11] A. Hime *et al.,* "Fundamental Symmetries with Trapped Atoms," Los Alamos Directed Research and Development Proposal, 1999; H. Behrens *et al.,* Ann. Phys. (N.Y.) **115**, 276 (1978).
[12] R. Guckert *et al.,* Phys. Rev. A **58**, R1367 (1998).
[13] C. J. Myatt *et al.,* Opt. Lett. **21**, 290 (1996).
[14] P. D. Lett *et al.*, J. Opt. Soc. Am. B **6**, 2084 (1989).
[15] R. B. Firestone *et al.,* in *Table of Isotopes,* edited by V. S. Shirley (Wiley, New York, 1996), 8th ed.
[16] A. Gorelov *et al.,* Hyperfine Interact. **127**, 373 (2000).